Removal of fluoride from drinking water using bimetallic nano-adsorbent MnFe$_2$O$_4$ prepared by chemical route

Julekha Khatun, Mrinal Kanti Adak and Debasis Dhak*

Nanomaterials Research Lab, Department of Chemistry, Sidho-Kanho-Birsha University, Purulia-723 104, West Bengal, India

E-mail: debasisdhak@yahoo.co.in, debasis_dhak.chem@skbu.ac.in

MnFe$_2$O$_4$ (MFO) bimetallic nano-adsorbents were prepared using chemical precursor decomposition method. Calcinations of the carbonaceous precursor mass at 700ºC, 4 h lead to the phase formation. The single crystalline cubic structure was confirmed by the X-ray diffraction study (XRD). The average crystallite size was 19 nm. Fourier transform infrared spectroscopy (FTIR) was performed both before and after the fluoride removal. Fluorinated aqueous solutions of 3 ppm, 5 ppm and 10 ppm were prepared to perform the fluoride removal tests. The adsorption times were considered to be 15 min, 30 min, 45 min and 60 min varying the adsorbent doses in the range from 0.05 g to 0.15 g for every 100 ml fluorinated aqueous solution. Almost 67% fluoride was removed using MFO with adsorbent dose 0.05 g/100 mL. The adsorption process occurred through chemi-adsorption process. The contact time and initial fluoride concentration were found to be very selective.

Keywords: Nano-adsorbent, drinking water, fluoride removal, chemical synthesis.

Introduction

Ground water is a primary source of drinking water and irrigation for more than 50% of the world population[1]. Along with the rapid increase of population and industrial activity more and more cases of groundwater contamination with inorganic pollutants are coming into the light day by day. Fluoride is one of such contaminant which is one of the greatest threats to human beings. The two main sources of fluoride in drinking water are natural i.e. geological and artificial i.e. man-made[2]. Among the two sources the major one is the geological one which contributes fluoride in large scale. Fluoride which is capable of mineralizing bones and tooth up to a certain level, however at its elevated level can give rise chronic toxicity. At its concentration beyond the standards it causes a fatal disease called "Fluorosis". Due to long term fluoride consumption in body also causes a long term damage to brain, kidney, liver, thyroid, lowers the haemoglobin level in blood resulting anaemia, muscle weakness, fatigue, pain in joints, polyurea are also the painful outcomes of fluorosis.

The World Health Organisation (WHO) guidelines suggests the maximum level of fluoride in drinking water is 1.5 mg/L, but the guideline varies differently for warm and cold weather, where according to the WHO suggestion the optimum level of fluoride concentration is 1.0 mg/L for warmer climates and 1.2 mg/L for cold climates[4]. Fluorosis has been reported as a fatal problem to 200 million people from among 25 nations all over the world[5]. India and China are worst affected. According to an estimate in India alone 62 million people including 6 million children are suffering from different types of health problem due to fluoride contaminated water[6]. Out of 32 states 17 states are seriously affected[7]. In West Bengal a total of 2.20 Lakhs people are affected. Malda, South 24 Paraganas and specially due to warm, dry climate, less availability of water Bankura, Purulia, Birbhum are the districts where fluorosis has spread its worst affects[8]. Thus the removal of fluoride from drinking water is great necessity in terms of both public health and environment.

The basic and conventional methods for fluoride removal are Membrane Separation[9], Ion exchange[10], Adsorption technique[11] and Coagulation-Precipitation. Nalgonda technique for fluoride removal is based on Coagulation-Precipitation technique which can remove at a low level (18–33%) including the release of toxic aluminium fluoride complexes[12], but due to very high level of contaminations, developing countries like China, Tanzania this technique has been success-

fully used both in individual and community levels[2]. In last two decades, researchers have reported nano sized adsorbents by deep route analysis of their properties at nano scale and found splendid result for the removal of fluoride contaminated in ground water[13]. This high defluoridation potential is due to their small size, large surface area, catalytic potential, large number of active sites, great ease of their separation and excellent reactivity[14]. Simplicity, low cost, safe operation, treatment stability[15] and most of all the high removal efficiency – these are the mysteries behind its world wide acceptance[16].

Ekka et al.[16] prepared an ionic liquid modified γ-alumina via modified sol gel method. Maximum adsorption capacity was found to be 25.0 mg/g from Langmuir isotherm at equilibrium fluoride concentration of 30 mg/L. Chen et al.[17] choose a coating granulation technology to remove excess fluoride from water. To enhance the performance capability they used latex/Fe-Al-Ce ratio of 0.5:1 at a temperature 65°C. These coated granules have the capacity to absorb 2.77 mg/g fluoride from water with an initial fluoride concentration of 0.001 M at pH 7. Zhang et al.[18] took the help of sorption method and used Zirconium-modified-Na-attapulgite (Zr-A) as adsorbent. They found it efficient over the pH range of 3.70–7.50. The fluoride adsorption property shows a good agreement with Langmuir model and exhibit a maximum capacity of 24.55 mg/g. Ma et al.[19] proposed the calcinations product (HTlc 500) of Mg-Al-Fe hydrotalcite compound for the fluoride sequestering purpose from water. In adsorption process metal oxides like iron, aluminium, and manganese oxides are widely used for water and wastewater treatments[20–22].

In the present study we reported the synthesis, characterization and fluoride absorption effectiveness of $MnFe_2O_4$ adsorbent. The effects of various parameters like adsorbent dose, initial fluoride concentration, contact time on the fluoride removal capacity of the synthesized adsorbent also reported here.

Materials and methods:

Materials:

Nanocrystalline $MnFe_2O_4$ was synthesized using precursor decomposition method. The chemicals required were $Mn(CH_3COO)_2.4H_2O$ [Merck Specialities Private Limited, Mumbai, ≥ 99.5%], $Fe(NO_3)_3.9H_2O$ [Merck Specialities Private Limited, Mumbai, ≥ 98%], Triethanol amine (abbreviated as TEA) [Merck Specialities Private Limited, Mumbai, ≥

99%], conc. HNO_3 [S.D. Fine Chemicals, India]. During the adsorption study double distilled water was used.

Preparation of the sorbent:

To synthesize the adsorbent, the solutions of $Mn(CH_3COO)_2.4H_2O$ and $Fe(NO_3)_3.9H_2O$ were taken in beaker in 1:2 ratio. Then appropriate amount of triethanol amine (TEA) (the total metal ion to TEA mole ratio is maintained at 1:3) was added to the mixture in excess to avoid precipitations of the metal ions. Here TEA acted as binding agent. Then the pH was adjusted to 5 using dilute nitric acid (1:1) and ammonium hydroxide (1:1). As a result a homogeneous precursor clear solution was obtained. The precursor solution was heated on a hot plate at a temperature 200°C. After complete dehydration a black, fluffy, carbonaceous mass was obtained. The obtained black mass was calcined at 700°C for 4 h in a muffle furnace. The overall synthesis procedure was given in Fig. 1 stepwise. The mechanism of the synthesis procedure was studied by Dhak et al.[23] in detail.
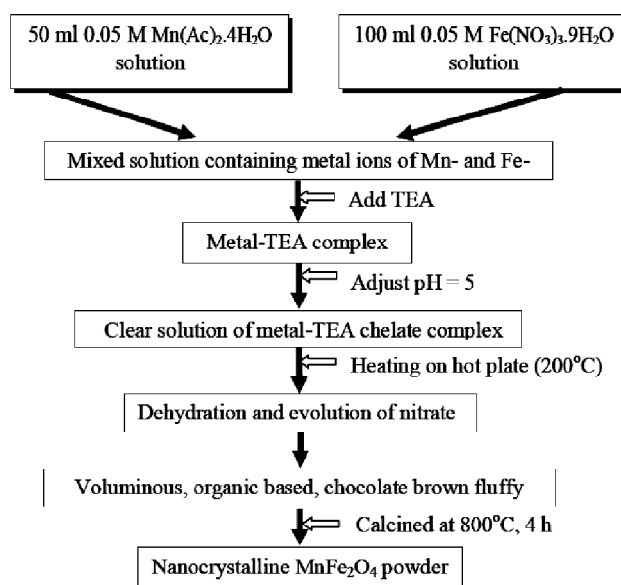

Fig. 1. Flow chart diagram for the preparation of $MnFe_2O_4$ nano-adsorbents.

Characterization of the materials:

Powder X-ray diffraction (XRD) study was done using BRUKER D8 ADVANCE eco in the scanning rate 2°/min in the 2θ range of 10° to 80°. Si crystal was used as a standard to calibrate the scanning angles and CuKα (λ = 1.5406 Å) was used as a target material. Fourier transform infrared

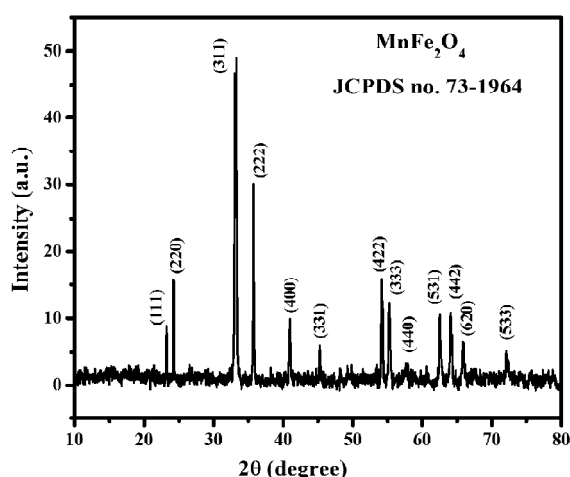spectroscopy (FTIR) (Perkin-Elmer, spectrum two) was used to study the characteristics absorption bands.

Batch adsorption experiments:

The adsorptions study was done using batch experiments. A known standard stock solution of fluoride was used to prepare 3 ppm, 5 ppm, and 10 ppm stock solutions. 100 ml of each solution was used to the batch experiments at different time intervals like 15 min, 30 min, 45 min, and 60 min. The adsorbent doses were 0.05 g/100 ml, 0.1 g/100 ml, and 0.15 g/100 ml. There are four steps that were involved in the sorption process. At the 1st step, the mixed definite quantities adsorbent with fluoride solution were shaken in the orbital shaker (Paragon RPM-0249, TXT-7203, India) with 150 rpm for the different time interval according to the batch. In the 2nd step, the solution after shaking was centrifuged at 2600 rpm for 10 min. 3rd step involved decantation and filtration of the fluoride solutions. The obtained solution was kept in plastic bottle and the fluoride concentration was measured using a fluoride meter adding require amount of TISAB-III (Thermo Orion Versa star Pro Advance Electrochemistry meter, Software Revision: r 4.06, Serial Number: V11855) (4th step).

Results and discussion

XRD study:

The X-ray diffraction pattern of $MnFe_2O_4$ was obtained after calcining the spinel at 700°C for 4 h. The pattern showed a single phase cubic structure which was in a good agreement to the JCPDS data file no. 73-1964. The *hkl* list was obtained with the help of WinPLOTR software (version: nov. 2013). The obtained lattice parameters were $a = b = c = 8.8$ Å, with 681.47 Å³ unit cell volume. The crystallite size of $MnFe_2O_4$ was calculated using Scherrer's formula as follows[24]

$$\text{Size } (D) = \frac{0.9\lambda}{\beta \cos \theta}$$

where β is the full width at half maximum of the diffraction peak and θ is the half angle of diffraction. The calculated average crystallite size was 19 nm. It is noteworthy to be mentioned that crystallite size is a measure of the size of coherently diffracting regions/domains of a material. Crystallite size is equal to grain size if the grain is perfectly single crystallite. However grains of sintered samples contains several dislocations and defects, which interrupt the periodicity of the crystalline nature so an individual grain may contain a number of crystallites defined as coherently diffracting regions. XRD technique provides the information of these crystallite (coherently diffracting region) size present in the grains.

FTIR study:

The FTIR study was done for precursor black mass and calcined powder at room temperature shown in Fig. 3. The characteristics absorption bands were observed at 3457, 1639, 532, 571 and 471 cm^{-1}. The bands at 3457 and 1639 cm^{-1} were responsible for O-H stretching and bending vibra-

Fig. 2. Powder X-ray diffraction pattern of $MnFe_2O_4$ calcined at 700°C for 4 h.
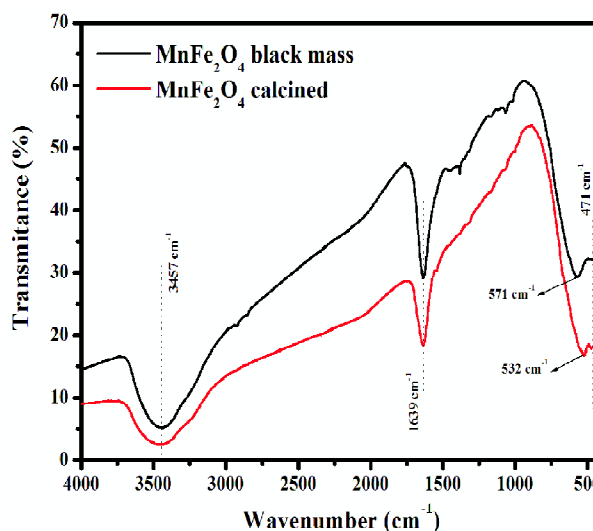
Fig. 3. Fourier transform infrared spectroscopy of $MnFe_2O_4$ (precursor black mass and calcined powder).

tion mode of water molecules[25]. The presence of water is due to the presence of moisture in the sample or in the sample compartment[26]. The peak observed at lower range i.e. near about 450 cm^{-1} was due to octahedral stretching of metal ion[27]. Between 1100–1200 cm^{-1} the small peaks observed were due to the O-O stretching frequency[28].

Effect on contact time on the adsorption of fluoride:

The sorption potential of the adsorbent material was depended on the contact time of the adsorbent with fluoride solution. Here the contact time was varied from 15 min to 60 min within a time interval of 15 min for 3 ppm, 5 ppm and 10 ppm fluoride solutions.

The variation of % of fluoride removal with contact time at the different adsorbent doses is given in Fig. 4. The figures showed that for 0.05 g and 0.1 g adsorbent doses the % of fluoride removal was increased from 15 min to 30 min after that it decreased slightly with increasing contact time.

But for 0.15 g adsorbent dose the % of fluoride removal decreased initially and followed an up down path. This type of trend could be explained by two ways. The first path stated, during the adsorption of fluoride ion the active surface area of the spinel decreased and the adsorption capacity was also decreased[29], whereas the second path considered that there is a repulsive force between the negatively charge fluoride ion that reduced the efficiency of the adsorbent and the adsorbed fluoride ion was released in solution[26]. The two paths might occur along with or individually.

So, from the Fig. 4 it was clear that the highest fluoride removal was observed for 0.05 g/100 ml and 0.1 g/100 ml adsorbent dose at a contact time of 30 min and 0.15 g/100 ml adsorbent dose at 45 min contact time.

Effect of adsorption dose on extent of fluoride removal:

The efficiency of the fluoride removal depends on the adsorption dose. In this parameter the adsorbent dose was
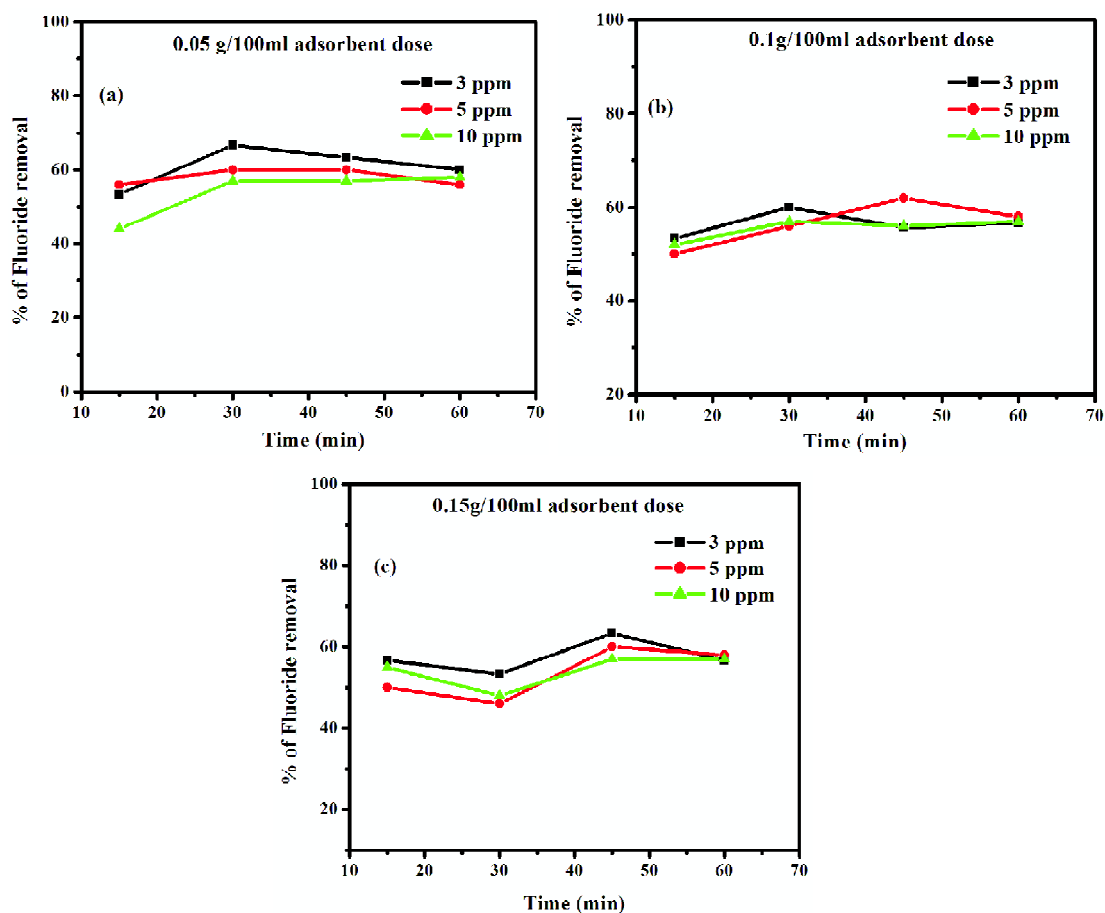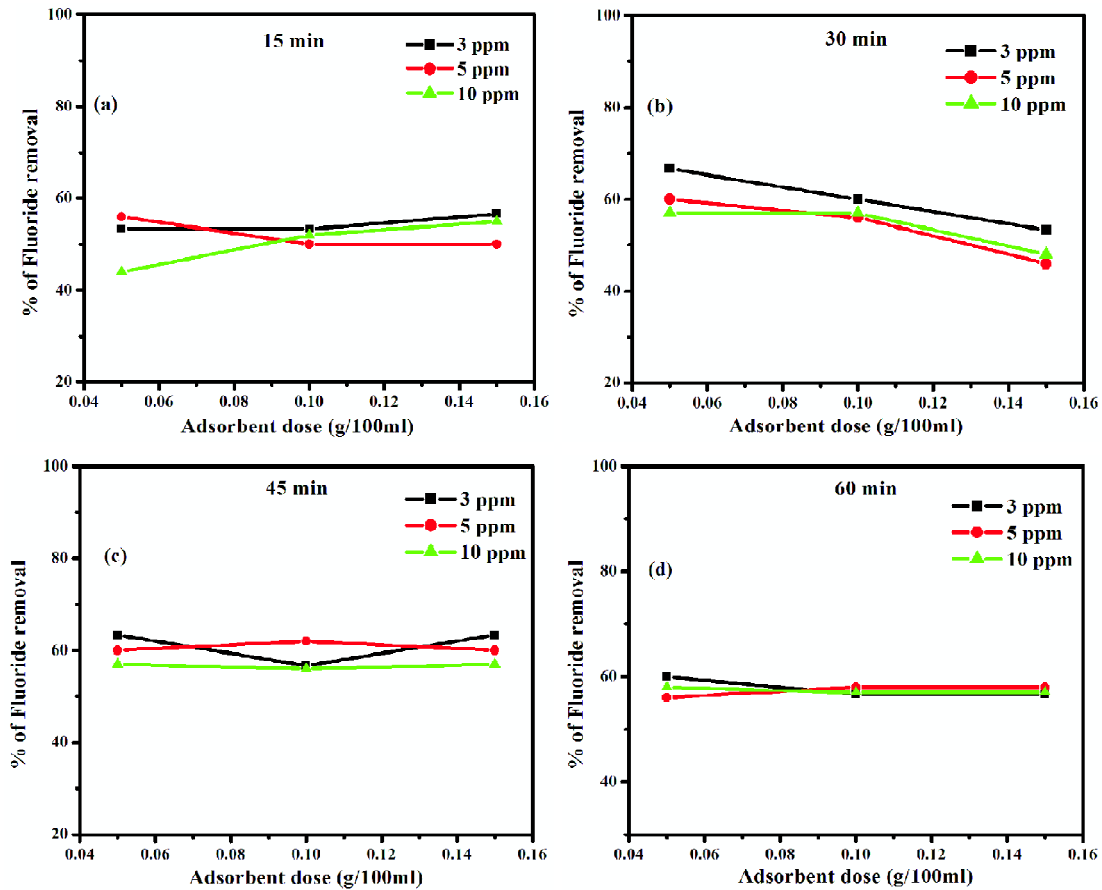

Fig. 4. % of fluoride removal vs contact time taking the adsorbent dose (a) 0.05 g/100 ml, (b) 0.1 g/100 ml, (c) 0.15 g/100 ml.

Table 1. Effect of fluoride removal as a function of contact time and adsorption doses

| Adsorbent dose (g/100 ml)	% of fluoride removal	3 ppm				5 ppm				10 ppm			
		15 min	30 min	45 min	60 min	15 min	30 min	45 min	60 min	15 min	30 min	45 min	60 min
0.05	removal	53	67	63	60	56	60	60	56	44	57	57	58
0.1		53	60	56	56	50	56	62	58	52	57	56	57
0.15		56	53	63	56	50	46	60	58	55	48	57	57

Fig. 5. % of fluoride removal vs adsorbent dose (g/100 ml) taking the contact times (a) 15 min, (b) 30 min, (c) 45 min and (d) 60 min.

varied from 0.05 g/100 ml, 0.1 g/100 ml, and 0.15 g/100 ml for the treatment of 3 ppm, 5 ppm, and 10 ppm fluoride solution using 15 min, 30 min, 45 min, and 60 min contact time.

Fig. 5(a-d) showed the percentage of fluoride removal with the variation of adsorption dose at different contact time. The figures show that the adsorption process does not follow the regular trend with increasing adsorbent dose. Here the high specific surface area and micro pore volume played a significant role in the adsorption process[26]. With increasing the adsorbent dose there was no significant increase of

% of fluoride removal. This was due to the overlapping of the active sites at higher doses. The adsorption might follow the mechanism[26] below:

$$MOH_{(S)} + H^+ \leftrightarrow MOH_2^+ \qquad (1)$$
$$MOH_2^+ + F^- \leftrightarrow MF_{(S)} + H_2O \qquad (2)$$
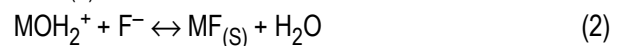
where, M and $MOH_{(S)}$ represent the metal ions (Fe^{3+} and Mn^{2+} in this case) and the surface hydroxyl group respectively. $MF_{(S)}$ indicates a surface site occupied by a fluoride ion. This is a type of chemi-adsorption process.

Conclusion

The nano-crystalline adsorbent MnFe$_2$O$_4$ was prepared using chemical precursor solution decomposition method. The XRD study showed a cubic structure and the average crystallite size was 19 nm calculated using Scherrer's formula. The characteristics band was observed during FTIR study. A systematic batch experiment was done by varying the contact time and adsorbent dose for 3 ppm, 5 ppm and 10 ppm fluoride solution. Almost 67% fluoride removal was achieved using 0.05 g/100 ml adsorption dose.

Acknowledgements

References

1. V. K. Rathore and P. Mondal, *Ind. Eng. Chem. Res.*, 2017, **56**, 8081.

2. M. K. Adak, B. Mondal, P. Dhak, S. Sen and D. Dhak, *Adv. Water Sci. Technol.*, 2017, **4**, 1.

3. S. Bibi, A. Farooqi, K. Hussain and N. Haider, *J. Clean. Prod.*, 2015, **87**, 882.

4. W. H. Organization, W. J. W. Supply and S. M. Programme, "Progress on sanitation and drinking water: 2015 update and MDG assessment", World Health Organization, 2015.

5. S. Ayoob and A. K. Gupta, *Crit. Rev. Environ. Sci. Technol.*, 2006, **36**, 433.

6. K. Brindha and L. Elango, *Fluoride Prop. Appl. Environ. Manag.*, 2011, 111.

7. C. B. Dissanayake, *Int. J. Environ. Stud.*, 1991, **38**, 137.

8. S. Rudra, *Analyst,* 2012, 2.

9. R. C. Maheshwari, *J. Hazard. Mater.*, 2006, **137**, 456.

10. K. Vaaramaa and J. Lehto, *Desalination*, 2003, **155**, 157.

11. C. Venkobachar, L. Iyengar and A. K. Mudgal, "Household defluoridation of drinking water using activated alumina", in: 'Proc. 2nd Int. Work. Fluorosis Prev. Defluoridation Water', ISFR, EnDeCo, Soborg, Denmark, 1997, pp. 138-145.

12. M. Habuda-Stanić, M. Ravančić and A. Flanagan, *Materials (Basel)*, 2014, **7**, 6317.

13. P. Chinnakoti, A. L. A. Chunduri, R. K. Vankayala, S. Patnaik and V. Kamisetti, *Appl. Water Sci.*, 2017, **7**, 2413.

14. I. Ali, *Chem. Rev.*, 2012, **112**, 5073.

15. A. Bhatnagar, E. Kumar and M. Sillanpää, *Chem. Eng. J.*, 2011, **171**, 811.

16. B. Ekka, R. S. Dhaka, R. K. Patel and P. Dash, *J. Clean. Prod.*, 2017, **151**, 303.

17. L. Chen, T.-J. Wang, H.-X. Wu, Y. Jin, Y. Zhang and X.-M. Dou, *Powder Technol.*, 2011, **206**, 291.

18. G. Zhang, Z. He and W. Xu, *Chem. Eng. J.*, 2012, **183**, 315.

19. W. Ma, N. Zhao, G. Yang, L. Tian and R. Wang, *Desalination*, 2011, **268**, 20.

20. P. Delaney, C. McManamon, J. P. Hanrahan, M. P. Copley, J. D. Holmes and M. A. Morris, *J. Hazard. Mater.*, 2011, **185**, 382.

21. D. E. Giles, M. Mohapatra, T. B. Issa, S. Anand and P. Singh, *J. Environ. Manage.*, 2011, **92**, 3011.

22. S. S. Tripathy and A. M. Raichur, *J. Hazard. Mater.*, 2008, **153**, 1043.

23. D. Dhak and P. Pramanik, *J. Am. Ceram. Soc.*, 2006, **89**, 1014.

24. B. D. Cullity and S. R. Stock, "Elements of X-ray Diffraction", 3rd ed., Pearson New International Edition, 2014.

25. M. K. Adak, A. Mukherjee, A. Chowdhury, U. K. Ghorai and D. Dhak, *J. Alloys Compd.*, 2018, **740**, 203.

26. M. K. Adak, A. Sen, A. Mukherjee, S. Sen and D. Dhak, *J. Alloys Compd.*, 2017, **719**, 460.

27. A. Mary Jacintha, A. Manikandan, K. Chinnaraj, S. Arul Antony and P. Neeraja, *J. Nanosci. Nanotechnol.*, 2015, **15**, 9732.

28. M. K. Adak, A. Mukherjee, A. Chowdhury, J. Khatun, U. K. Ghorai and D. Dhak, *J. Mater. Sci. Mater. Electron.*, 2018, **29**, 15847.

29. S. S. Tripathy, J.-L. Bersillon and K. Gopal, *Sep. Purif. Technol.*, 2006, **50**, 310.